



Cite this: *Biomater. Sci.*, 2022, **10**, 6399

## Dynamic covalent crosslinked hyaluronic acid hydrogels and nanomaterials for biomedical applications

Shujiang Wang,<sup>a</sup> Shima Tavakoli,<sup>a</sup> Rohith Pavan Parvathaneni,<sup>a</sup> Ganesh N. Nawale, <sup>a</sup> Oommen P. Oommen, <sup>b</sup> Jöns Hilborn<sup>a</sup> and Oommen P. Varghese <sup>a</sup>

Hyaluronic acid (HA), one of the main components of the extracellular matrix (ECM), is extensively used in the design of hydrogels and nanoparticles for different biomedical applications due to its critical role *in vivo*, degradability by endogenous enzymes, and absence of immunogenicity. HA-based hydrogels and nanoparticles have been developed by utilizing different crosslinking chemistries. The development of such crosslinking chemistries indicates that even subtle differences in the structure of reactive groups or the procedure of crosslinking may have a profound impact on the intended mechanical, physical and biological outcomes. There are widespread examples of modified HA polymers that can form either covalently or physically crosslinked biomaterials. More recently, studies have been focused on dynamic covalent crosslinked HA-based biomaterials since these types of crosslinking allow the preparation of dynamic structures with the ability to form *in situ*, be injectable, and have self-healing properties. In this review, HA-based hydrogels and nanomaterials that are crosslinked by dynamic-covalent coupling (DCC) chemistry have been critically assessed.

Received 22nd July 2022,  
Accepted 12th September 2022

DOI: 10.1039/d2bm01154a

rsc.li/biomaterials-science

## 1. Introduction

The ECM is a complex three-dimensional (3D) microenvironment that consists of proteins, glycoproteins, and polysaccharides, secreted locally by cells.<sup>1</sup> It provides structural, biochemical, and biophysical support for cells, and any alteration in the ECM properties can affect cellular behavior. Moreover, the ECM supports tissue integrity and elasticity, and plays a critical role in tissue regeneration, as well as promotes tissue healing. Thus, there is an increasing demand to tailor biomaterials that mimic the natural ECM and provide a suitable microenvironment for cells including stem cells, similar to the natural stem cell niche. Hydrogels based on ECM components have been extensively developed for biomedical applications such as *in vitro* disease modeling, 3D cell culture platforms, scaffolds for tissue engineering, drug delivery systems, and biosensors.<sup>2</sup> Since HA is one of the major components in the ECM, hydrogels using this biopolymer are of great interest. HA is composed of D-glucuronic acid and N-acetyl-D-glucosamine

and is abundant in the ECM of connecting tissues, synovial fluid of joints, and the dermis layer of the skin.<sup>3,4</sup> Within the ECM, HA plays a vital role in sequestering proteins that are produced by cells, and often HA with a very high molecular weight (up to 10 000 kDa)<sup>5</sup> can be found. Commercially, HA is isolated from rooster comb or genetically engineered bacteria and are purified and degraded to yield HA fragments with different molecular weights. High molecular weight HA plays an important role in maintaining cell integrity, cell-cell communication, hydration, and tissue integrity *in vivo*, and it exhibits anti-angiogenic and anti-inflammatory properties,<sup>6,7</sup> however, upon injury or inflammation, the ubiquitous hyaluronidase enzyme expression is upregulated that degrades high molecular weight HA into low molecular weight HA (<100 kDa), which exhibits pro-inflammatory, immune-stimulatory, and angiogenic characteristics<sup>8</sup> that stimulate wound healing. These size-dependent effects of HA allow the tailoring of materials for different applications. *In vivo*, HA is degraded enzymatically using a ubiquitous enzyme hyaluronidase and by oxidative processes; however, high molecular weight HA could also be hydrolyzed under acidic or basic conditions.<sup>5</sup> Interaction of HA with cells is regulated by molecular interactions with specific cell surface receptors such as CD44, RHAMM (receptor for hyaluronan mediated motility), LYVE-1 (lymphatic vessel endothelial receptor-1), and TLR-4 (toll-like

<sup>a</sup>Macromolecular Chemistry Division, Department of Chemistry-Ångström Laboratory, Uppsala University, 751 21 Uppsala, Sweden.

E-mail: oommen.varghese@kemi.uu.se

<sup>b</sup>Bioengineering and Nanomedicine Group, Faculty of Medicine and Health Technologies, Tampere University, 33720 Tampere, Finland



receptor-4).<sup>9</sup> CD44 is also a known cancer stem cell marker which makes them ideal candidates for developing targeted drug delivery systems. Several HA-based nanoparticles and molecular conjugates have been employed to deliver drug molecules to CD44-positive cancer cells with high selectivity. It was recently shown that HA also forms self-assembled nanoparticles with RNA molecules by hydrophobic interactions, suggesting the potential role of such ECM components in stabilizing circulating RNA molecules *in vivo*.<sup>10</sup>

To design HA-based biomaterials, both chemical and physical crosslinking methods have been explored.<sup>11,12</sup> Physical interactions, including ionic interactions, chain entanglement, electrostatic interactions, hydrogen bonds, van der Waals interactions, or hydrophobic self-assembly, have been considered as physical crosslinking for HA hydrogels.<sup>13,14</sup> Physical crosslinking results in a rapid gelling process, and it avoids the usage of toxic catalysts or crosslinkers. However, the dynamic polymer network formed by physical or ionic crosslinking undergoes disassembly upon swelling or by a competitive ionic interaction with salts or negatively charged biopolymers such as heparan sulfate in the biological milieu.<sup>15</sup> Chemically crosslinked HA hydrogels, such as with 1,4-butanediol di-(propan-2,3-diolyl) ether crosslinks, on the other hand, form stable 3D networks that are normally considered “permanent” and not reversible bonds (Fig. 1). These permanently cross-linked biomaterials are used to develop aesthetic products in the cosmetic industry, such as volumetric dermal fillers (*e.g.*, Restylane Lift® distributed by Galderma and Juvéderm® Volift, and Juvéderm® Ultra Smile from Allergan). Hydrogels based on dynamic covalent coupling (DCC) chemistry have a reversible and adaptable polymer network, which allows the

development of hydrogels with tuneable physical and mechanical characteristics, and stimuli responsive properties (*e.g.* shear-thinning and self-healing properties).<sup>16</sup> The DCC reaction is a dynamic process that allows the exchange of molecular components at equilibrium to achieve thermodynamic minima of the system.<sup>17</sup> This reaction includes esterification, imine, hydrazone, and oxime formation, Diels–Alder reactions, disulfide exchange reactions, and boronic ester formation.<sup>18</sup> DCC has been widely used for developing HA gels as it provides a mild, efficient, and biocompatible strategy that does not release toxic by-products. In different studies, dynamic covalent bonded hydrogels have been used to develop materials with shear-thinning and self-healing properties with tuneable physical and mechanical characteristics.<sup>16</sup> However, most of these dynamic processes showed slow formation and exchange. Although the dynamic gelation process can be accelerated by increasing the polymer concentration, adding a catalyst, or by tuning the pH, these methods compromise the biocompatibility of the hydrogels. Therefore, HA-derived hydrogels that undergo fast and efficient bioorthogonal DCC without any toxic catalysts, or UV light under physiological conditions have been greatly employed for different biomedical applications.

The present review aims to give an up-to-date overview of HA-based hydrogels and nanomaterials that have been developed employing DCC. For this purpose, we first discuss the chemical aspects of such reactions that modulate the coupling efficiency under physiological conditions, and then we discuss the scope and limitations of HA hydrogels and nanoparticles formed by DCC for different biomedical applications.

## 2. DCC in HA hydrogels

Hydrogels are 3D networks produced from hydrophilic (macro) molecules which can maintain a large amount of water in their structures.<sup>19</sup> These crosslinked polymer networks with high water contents and rheological solid-like properties are attractive materials for biomedical applications.<sup>20,21</sup> Some hydrogels that are synthesized by dynamic bonds can undergo different structural changes in response to a given stimulus by reversibly forming and breaking covalent bonds. These hydrogels are commonly described as “dynamic hydrogels”.<sup>17</sup> Dynamic hydrogels can be responsive to different stimuli such as light, temperature, pH, ligands, or biomolecules.<sup>19</sup>

Several natural and synthetic polymers have been utilized to synthesize hydrogels for biomedical applications. Hydrogels derived from ECM-based polymers mimic ECM characteristics and have received significant attention as they can support different cellular functions.<sup>22,23</sup> Among various types, HA is widely used for engineering hydrogels for bio-applications, due to its bio-functionality, as well as due to the availability of reactive functional groups (carboxylic acids and hydroxyls) that can be easily modified with different polymers, proteins, or small molecules to engineer functional materials with diverse bioactivity. HA hydrogels can be synthesized through covalent

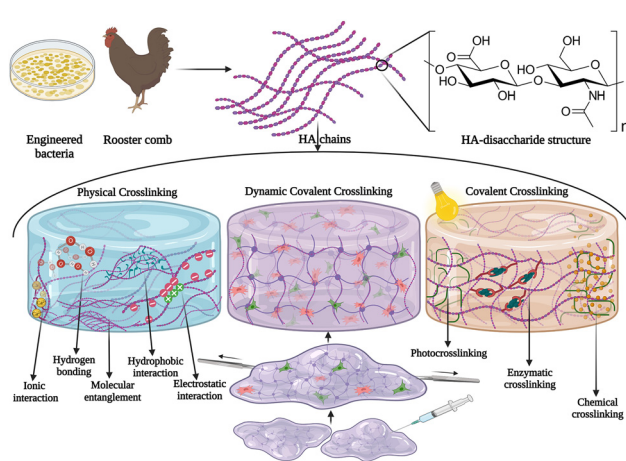


**Fig. 1** The schematic representative of HA chemical structure and hydrogels developed by different crosslinking chemistries. Physically formed HA hydrogels could be produced by ionic interactions, hydrogen bonding, chain entanglement, hydrophobic force, and electrostatic interactions. Dynamic bonded hydrogels developed by different chemistries have self-healing and self-recovery properties. This gel can be injectable and various cell types can be encapsulated inside the hydrogel. Chemically crosslinked hydrogels can be formed by photocrosslinking, and enzymatic and chemical crosslinking.



and non-covalent crosslinking.<sup>24</sup> Covalently crosslinked HA hydrogels are generally more stable than physical networks; static covalent bonds often result in more elastic materials, while physical hydrogels typically exhibit a more viscous behavior.<sup>25–27</sup> DCC reactions are intermediary crosslinking that can produce viscoelastic materials that stress relax and deform under stress which facilitates cellular functions such as spreading, proliferation, migration, and differentiation.<sup>18</sup> In general, HA hydrogels produced by DCC have self-healing properties due to the reversible nature of dynamic bonds. Self-healing hydrogels are particularly interesting because of their unique abilities to repair structural damage and recover the original functions, similar to the healing of natural tissues. Besides, self-healing with shear-thinning properties facilitates reversible sol–gel transitions that provide astonishing features to hydrogels to form injectable materials that could be potentially used as carriers for drug/cell delivery or for developing bioinks for 3D printing. Therefore, self-healing HA hydrogels as biomedical materials have received rapidly growing attention in recent years.<sup>20</sup> Several studies have reported the use of dynamic covalent crosslinking strategies to engineer HA-based hydrogels for various bio-applications, as summarized in Table 1.

The DCC involves reversible bond formation and bond cleavage under thermodynamic control. The equilibrium and kinetics of the DCC can be affected by substrate structure and reaction conditions, such as solvent, temperature, pH, or ionic strength.<sup>18,25</sup> To develop an ECM mimetic hydrogel for living cells and tissues, the DCC is preferred to be performed at neutral pH, to be tolerable by cells and tissues. The most investigated DCC chemistry, including the formation of imine, oxime, hydrazone, disulfide, and boronic ester products, and the Diels–Alder reaction (Fig. 2) that has been employed are summarized below.

## 2.1. Imine reaction (Schiff-base)

The Schiff-base reaction is among the most utilized cross-linking reactions for ECM hydrogel formation.<sup>31</sup> It involves the nucleophilic addition of an amine to an aldehyde or a keto substrate, followed by water elimination to form the imine product.<sup>19</sup> The reaction is compatible with aqueous conditions and water is the only by-product that makes this reaction suitable for numerous biomedical applications. Hydrogels produced with imine bonds possess self-healing properties because the imine reaction undergoes reversible imine–amine exchange. Hydrogels based on this chemistry have been evaluated for different biomedical applications. For instance, aldehyde-functionalized HA and the non-ECM component, *N*,*O*-carboxymethyl chitosan, were employed for abdominal tissue regeneration, and were evaluated in a rat model with an open abdomen and abdominal wall defect.<sup>32</sup> The rats treated with the HA/chitosan gel showed a rapid cellular response, sufficient ECM deposition, and marked neovascularization. A shortcoming of imine crosslinked gels is, however, the requirement of acidic pH for the crosslinking reaction and the poor hydrolytic stability of the imine bonds. This leads to faster degradation and swelling of the hydrogels. Furthermore, the

released aldehyde-functionalized polymer can interact with the surrounding tissue and interfere with the biological process *in vivo*.<sup>33,34</sup> This side reaction can also affect the crosslinking density of the hydrogel and accelerate hydrogel degradation.

## 2.2. Oxime and hydrazone formation

Oxime and hydrazone-based hydrogel products require a condensation reaction between polymers having hydrazide or alkoxyamine derivatives and aldehyde or ketone substrates, generating water as a byproduct. Unlike imine reactions, these nucleophilic reagents (hydrazide and aminoxoy) have an electronegative heteroatom (N or O) at the alpha position, which significantly changes the reactivity of nucleophiles and that of the obtained products.<sup>35</sup> Additionally, contrasting the amine functional group, which is basic ( $pK_a > 9$ ), the hydrazide and oxime residues are acidic ( $pK_a \approx 4.5$ ), which makes them more nucleophilic. For this reason, hydrazone and oxime formation reactions are efficient, selective under mild reaction conditions, and provide crosslinks with greater intrinsic hydrolytic stability as compared to imines.<sup>36</sup> Both the reactions are reversible in an aqueous environment and the hydrolysis occurs swiftly at acidic pH.<sup>35</sup> Therefore, careful selection of the reacting substrates is important for the enhancement of the hydrolytic stability of hydrazone and oxime bonds. It is well known that hydrazone and oxime generally exhibit better hydrolytic stability than imines due to the alpha effect.<sup>36</sup> We have previously developed a novel hydrazone-crosslinked HA hydrogel using carbodihydrazide (CDH) as the hydrazide moiety for hydrazone crosslinking with HA aldehyde as a substrate, which was utilized for delivering therapeutic protein namely, recombinant human bone morphogenetic protein-2 (rhBMP-2), which exhibited extraordinary hydrolytic and enzymatic stability with good mechanical strength and low swelling ratio, resulting in efficient bone formation *in vivo*.<sup>37</sup> Compared to conventional hydrazone crosslinking (*e.g.*, using adipic acid-derived hydrazide (ADH)) CDH-mediated hydrazone crosslinking displayed 15-fold higher stability at pH 5. This exceptional hydrolytic stability was attributed to the resonance-stabilization of the  $N^2$  positive charge during the formation of a hydrazone bond (Fig. 3a and b). Additionally, the *in vivo* evaluation of this hydrogel revealed neo-bone with a highly ordered collagen matrix mimicking natural bone regeneration (Fig. 3d and e). Moreover, it is interesting to note that besides the structure of nucleophiles, electrophilic carbonyl functionality also influences the hydrolytic stability of hydrazone and oxime linkages. Hydrazone obtained from the keto substrate possesses enhanced hydrolytic stability as compared to the corresponding aldehyde, and aromatic aldehyde forms a more stable oxime than aliphatic aldehydes/ketones.<sup>35,38</sup>

However, the reaction employing ketone or aromatic aldehydes as electrophiles is much slower than the aliphatic aldehyde-based reaction, especially when the reaction is performed at neutral pH.<sup>35</sup> The slow reaction rate under physiological conditions limits the use of hydrazone and oxime crosslinking for many biological applications.<sup>39,40</sup> It has, however, been demonstrated that the hydrazone and oxime reaction rate



**Table 1** DCC strategies to engineer HA-based hydrogels for various bio-applications

No.	Main component	DCC type	Application	Reference
1	Aldehyde-functionalized HA and methacrylate chitosan	Schiff base	Injectable scaffolds for cell transplantation	Han <i>et al.</i> <sup>101</sup>
2	Aldehyde-modified HA and cystamine dihydrochloride	Schiff base	Drug delivery and tissue regeneration	Li <i>et al.</i> <sup>102</sup>
3	Aldehyde-modified HA and carboxyethyl-modified chitosan	Schiff base	Drug delivery	Qian <i>et al.</i> <sup>103</sup>
4	Oxidized HA and glycol chitosan, and adipic acid dihydrazide	Schiff base and hydrazone	3D bioprinting	Kim <i>et al.</i> <sup>104</sup>
5	Aldehyde-modified HA and hydrazide-functionalized poly ( $\gamma$ -glutamic acid)	Schiff base	Load-bearing tissue engineering	Ma <i>et al.</i> <sup>105</sup>
6	Aldehyde-modified HA and collagen	Schiff base	Cartilage engineering	Kong <i>et al.</i> <sup>106</sup>
7	Aldehyde-modified HA and <i>N</i> -succinyl-chitosan	Schiff base	Injectable biomaterial	Sun <i>et al.</i> <sup>107</sup>
8	Aldehyde-modified HA and amino-modified HA	Schiff reaction	Injectable biomaterial	Tan <i>et al.</i> <sup>108</sup>
9	Oxidized HA and adipic acid dihydrazide	Schiff base	3D bioprinting	Weis <i>et al.</i> <sup>109</sup>
10	Aldehyde-modified HA and <i>N</i> -succinyl-chitosan	Schiff base	Cartilage engineering	Tan <i>et al.</i> <sup>110</sup>
11	Monoaldehyde-modified HA and carbohydrazide-modified gelatin	Schiff base	Injectable biomaterial	Hozumi <i>et al.</i> <sup>111</sup>
12	Alkoxyamine-terminated pluronic F127 (AOP127) and oxidized HA	Oxime	Anti-adhesion barrier	Li <i>et al.</i> <sup>112</sup>
13	Hydrazine-modified elastin-like protein and aldehyde-modified HA	Hydrazone	Cell delivery	Wang <i>et al.</i> <sup>113</sup>
14	Acylhydrazone or oxime HA	Hydrazone and oxime	Bioconjugation	Wang <i>et al.</i> <sup>50</sup>
15	Aldehyde-modified HA and hydrazine-modified elastin-like protein	Hydrazone	Cartilage regeneration	Zhu <i>et al.</i> <sup>114</sup>
16	Aldehyde-modified HA and hydrazide-modified HA	Hydrazone	3D bioprinting	Wang <i>et al.</i> <sup>115</sup>
17	Adipic dihydrazide-modified HA and dialdehyde-modified-pectin	Hydrazone	Cartilage engineering	Chen <i>et al.</i> <sup>116</sup>
18	Hydrazide modified HA and benzaldehyde terminated F127 triblock polymers	Hydrazone	Wound healing	Li <i>et al.</i> <sup>117</sup>
19	Hydrazine-modified HA and aldehyde-modified HA and catalysts	Hydrazone	Injectable biomaterial	Lou <i>et al.</i> <sup>49</sup>
20	Carbohydrazide-modified carboxymethyl cellulose and aldehyde-modified HA	Hydrazone	3D bioprinting	Janarthanan <i>et al.</i> <sup>118</sup>
21	Aldehyde and hydrazide-modified HA	Hydrazone	Protein delivery	Paidikondala <i>et al.</i> <sup>51</sup>
22	Gallop and hydrazide-modified HA, and aldehyde-modified HA	Hydrazone	Immunosuppressive tissue adhesive	Samanta <i>et al.</i> <sup>53</sup>
23	Norbornene-modified HA and aldehyde or hydrazide-modified HA	Hydrazone	3D printing	Muir <i>et al.</i> <sup>119</sup>
24	Aldehyde and furan-modified HA with bis(oxamine) PEG and modified peptide	Oxime and Diels-Alder	3D cell culture	Baker <i>et al.</i> <sup>120</sup>
25	S-protected thiolated-HA	Disulfide	3D cell culture	Asim <i>et al.</i> <sup>121</sup>
26	Thiolated-HA and PEGDA	Disulfide	Cardiac tissue engineering scaffold	Young <i>et al.</i> <sup>122</sup>
27	Thiolated-HA and gold nanoparticles	Disulfide	3D bioprinting	Skardal <i>et al.</i> <sup>123</sup>
28	Thiolated-HA	Disulfide	3D cell culture	Bian <i>et al.</i> <sup>124</sup>
29	Thiolated-HA	Disulfide	Soft biomaterial	Wu <i>et al.</i> <sup>125</sup>
30	Thiolated-HA and acrylated-HA	Disulfide	Injectable biomaterial	Cao <i>et al.</i> <sup>126</sup>
31	Thiol- and hydrazide-modified HA and oxidized alginate	Disulfide and hydrazone	Drug release	Zhang <i>et al.</i> <sup>127</sup>
32	Thiolated-HA and thiolated-carboxymethyl cellulose	Disulfide	Drug release	Deng <i>et al.</i> <sup>128</sup>
33	Pyridyl disulfide-modified HA and macro-crosslinker PEG-dithiol	Disulfide	Protein delivery and cell encapsulation	Choh <i>et al.</i> <sup>129</sup>
34	Aldehyde modified-HA and 3,3'-dithiobis (propionic hydrazide)	Disulfide (in the crosslinker)	Tissue adhesive	Sigen <i>et al.</i> <sup>130</sup>
35	Furan and dopamine hydrochloride, and 3-aminophenylboronic acid-modified HA	Diels-Alder and boronate ester	Cartilage regeneration	Yu <i>et al.</i> <sup>131</sup>
36	Furan-ADH modified HA and furan-aldehyde modified HA	Diels-Alder	Tissue adhesive	Yu <i>et al.</i> <sup>132</sup>
37	Furan and tyramine-modified HA and maleimide-modified PEG	Diels-Alder	Cartilage engineering	Yu <i>et al.</i> <sup>133</sup>
38	HA-furan-adipic dihydrazide and HA-furan-aldehyde	Diels-Alder	Growth factor delivery	Hu <i>et al.</i> <sup>134</sup>
39	Furan-modified HA and maleimide-PEG	Diels-Alder	Cartilage engineering	Wang <i>et al.</i> <sup>135</sup>
40	Norbornene modified-HA and methyltetrazine modified-HA	Diels-Alder	3D cell culture	Delplace <i>et al.</i> <sup>136</sup>
41	HA modified with benzoxaborole	Boronic ester	Injectable scaffolds for tissue engineering and cell therapy	Figueiredo <i>et al.</i> <sup>137</sup>
42	Phenylboronic acid-modified HA and poly (vinyl alcohol)	Boronic ester	Drug delivery, 3D cell culture, and 3D bioprinting	Shi <i>et al.</i> <sup>138</sup>
43	3-Aminophenylboronic acid-modified HA and a saccharide	Boronic ester	Drug delivery	Oliveira <i>et al.</i> <sup>139</sup>
44	Boronic acid-modified HA and fructose-modified HA	Boronic ester	Injectable biomaterial	Figueiredo <i>et al.</i> <sup>140</sup>
45	Boronic acid-modified HA and maltose-modified HA	Boronic ester	Soft biomaterial	Tarus <i>et al.</i> <sup>141</sup>



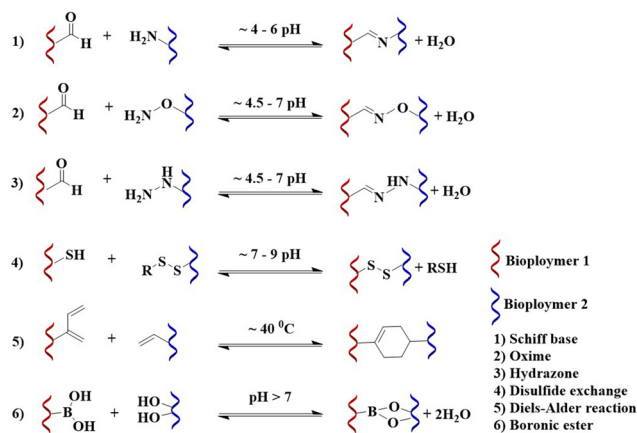


Fig. 2 Chemical schematic and reaction conditions for the formation of imine,<sup>28</sup> oxime,<sup>29</sup> hydrazone,<sup>29</sup> disulfide,<sup>30</sup> Diels–Alder,<sup>18</sup> and boronic ester<sup>12</sup> reactions.

increases significantly by introducing electron-withdrawing substituents to electrophilic substrates, such as *ortho*-boronic acid and nearby acid or basic groups.<sup>41,42</sup>

The nucleophilicity of the reactant also influences the reaction kinetics. In general, hydrazone formation is faster than oxime formation, and reactions involving hydrazone substituents with a nearby acidic group provide higher reactivity.<sup>41</sup> McKinnon *et al.* designed a bis-aliphatic hydrazone-linked hydrogel that forms most rapidly at physiological pH rather than at acidic pH without requiring aniline catalysis.<sup>43</sup> Besides modifying the substrate structure, catalysts have also been used to accelerate hydrazone and oxime formation. The most popular catalyst is aniline which promotes hydrazone and oxime conjugation at pH 7 by lowering the activation energy required for the rate-limiting dehydration step.<sup>44</sup> This catalyst has wide application in bioconjugation for biomolecule modification, labeling, drug design, and delivery, and it has also been used for hydrogel synthesis. However, it is known that aniline catalysis in hydrazone/oxime formation is less efficient at physiological pH as compared to acidic pH. For example, 100 mM aniline lead to a 400-fold reaction rate increase at pH 4.5, while the rate increase is only ~40-fold at neutral pH.<sup>44</sup> In addition, aniline requires a large quantity (above millimolar scale) as compared to the low substrate concentration (micro-molar scale) in many bioconjugation applications) to promote

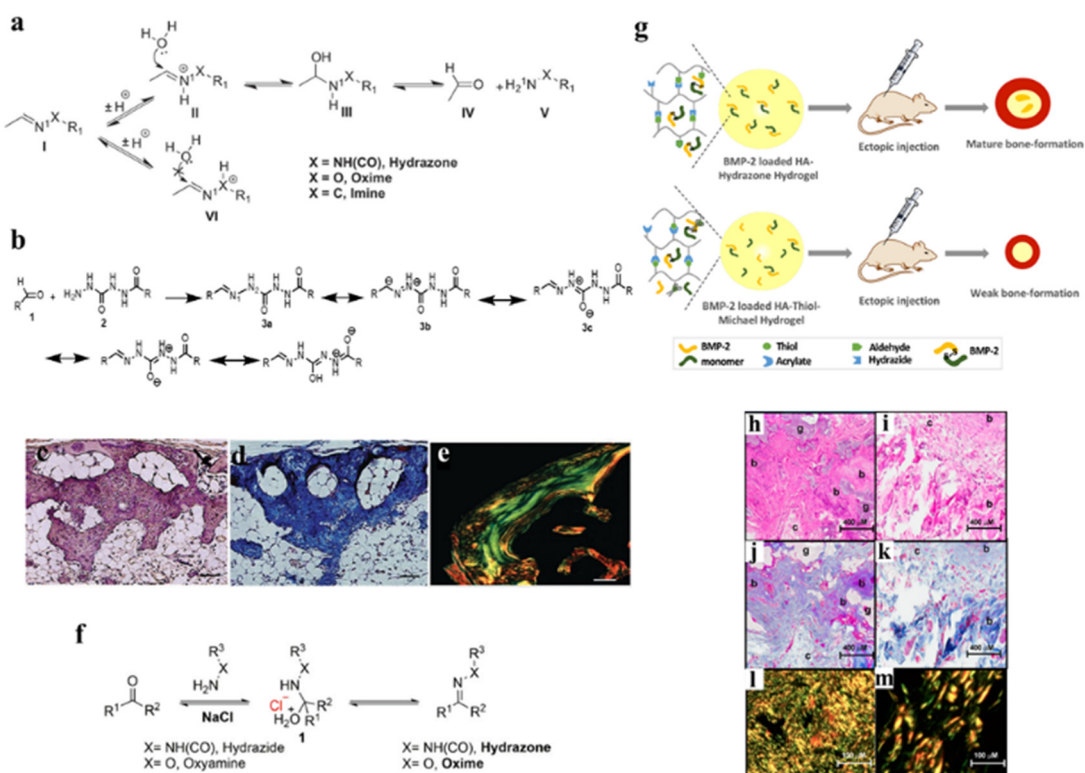


Fig. 3 (a) Hydrolysis mechanism of hydrazone, oxime, and imine, (b) the chemical schematic of the major resonance structure of the CDH hydrazone, (c–e) histological examination of ectopic bone harvested after 7 weeks post-implantation stained with hematoxylin/eosin (H&E), Masson's trichrome, and picrosirius red, respectively,<sup>37</sup> (f) reaction scheme of the salt stabilized transition state for hydrazone and oxime formation,<sup>50</sup> (g) HA-hydrazone and HA-thiol–Michael hydrogels containing rhBMP-2 indicating different bone forming profiles after ectopic implantation of the hydrogels, (h and i) histological evaluation of hematoxylin/eosin (H&E) stained cross sections of bone tissue obtained with HA-hydrazone hydrogels and HA-thiol–Michael hydrogels, respectively, (j and k) Masson's trichrome staining of cross sections of bone tissue obtained with HA-hydrazone hydrogels and HA-thiol–Michael hydrogels, and (l–m) collagen thickness in neobone after picrosirius red staining of cross sections of bone tissue as observed with a polarized light microscope with HA-hydrazone hydrogels and HA-thiol–Michael hydrogels.<sup>51</sup>



the reaction at a reasonable rate. Therefore, several aniline analogs are designed to achieve higher catalytic efficiency.<sup>35</sup> Recently, a self-immolation approach using aniline derivatives was used to accelerate hydrazone-cross-linked hydrogel formation.<sup>45</sup> In this study, the aniline released from the proaniline in the presence of  $H_2O_2$  and *in situ* leads to an instant increase in the rate of hydrazone formation by 10-fold. The substitutions on the aryl ring of aniline for the enhancement rate of the reaction are also reported.<sup>44,46,47</sup> Aniline analogs substituted with electron-donating groups have shown enhanced catalysis at neutral pH as compared to aniline, and aniline derivatives with *ortho*-proton donors that have  $pK_a$  values closest to neutral have been reported with the highest catalytic efficiency.<sup>48</sup>

Despite the catalytic efficiency, the major disadvantage of aniline and aniline analogs includes cytotoxicity for bio-applications and poor water solubility. Thus, other types of biocompatible catalysts are highly demanded for the synthesis of hydrogels with biomedical applications. Sulfonated amino-benzimidazole has been reported as a cyocompatible catalyst that has been utilized to develop hydrogels with both high injectability and stability for biomedical applications.<sup>49</sup> We have recently developed non-nucleophilic catalysts, such as carboxylate and aqueous salt solution, which exhibited significant enhancement in the catalysis of hydrazone/oxime-based hydrogel crosslinking with aldehyde and keto substrates at physiological pH.<sup>50</sup> The addition of different types of salts can increase the reaction rate for hydrazone and oxime formation by  $\approx 5\text{--}7$  fold at physiological pH by stabilizing the rate-limiting transition state as well due to the '*salting out effect*' that increases the local concentration of the substrates under aqueous conditions.<sup>50</sup> Fig. 3f shows the reaction mechanism for hydrazone and oxime formation at neutral pH that involves the formation of a charged intermediate 1, followed by a dehydration step which is the rate-limiting step.<sup>50</sup>

Evaluation of the bioactivity of the ECM mimetic hydrogel as a result of crosslinking chemistry or the conjugation of bioactive molecules is also crucial for tailoring functional 3D scaffolds. We have recently evaluated the effect of crosslinking chemistry of HA hydrogels on the *in vitro* and *in vivo* bioactivity of rhBMP-2.<sup>51</sup> In this regard, two different hydrogels including hydrazone crosslinked and thiol-Michael addition crosslinked HA hydrogels were developed. Both the hydrogels revealed similar physical and mechanical properties. However, they showed differences in the biological activity of BMP-2 in both *in vitro* and *in vivo* experiments. Subcutaneous implantation of the two hydrogel systems encapsulated with identical BMP-2 concentrations in a rat model demonstrated a clear difference in bone formation. In the hydrazone crosslinked hydrogel, the volume of formed bone was significantly higher as compared to the HA-thiol-Michael hydrogel (Fig. 3g). The differences in bone formation were also reflected in the quality of bone with hematoxylin & eosin (H & E) and Masson's trichrome staining of the newly formed tissue indicated better quality bone formation with osteoblasts and connective tissue in the HA-hydrazone hydrogel group as compared to the HA-thiol-Michael

hydrogel group (Fig. 1h-m). These results suggest that reactive functional groups such as thiols in a hydrogel may interact with the tertiary structure of the encapsulated protein to affect the biological outcome. The bioactivity of HA-based hydrogels could be easily manipulated by conjugating other bioactive molecules. Recently, covalent grafting of the dopamine moiety to a hydrazone crosslinked HA-chondroitin sulfate composite hydrogel was reported to form a brain-mimetic 3D scaffold that promotes neuronal network formation.<sup>52</sup> Similarly, grafting of gallic acid to the HA hydrogels rendered immunosuppressive characteristics by polarizing macrophages to the M2 phenotype and displayed antioxidant properties.<sup>53</sup>

### 2.3. Disulfide exchange

The disulfide exchange reaction involves a nucleophilic substitution reaction between an active disulfide and a thiolate ion which leads to the liberation of another thiolate ion. Although this reaction is highly selective, the reaction product remains sensitive to free thiols and dissolved oxygen in the system. The disulfide bonds are, however, stable in the presence of other nucleophiles and exhibit high resistance towards hydrolysis. Though the reaction can be carried out over a broad range of pH, it is more favorable under basic conditions.<sup>54</sup> Normally the reaction is performed at pH  $> 9$  to ensure a sufficient amount of thiolate which is the key intermediate that drives the forward reaction. We have recently reported that by employing thiols with different  $pK_a$  values the reactivity for disulfide exchange reactions could be manipulated.<sup>30</sup> Disulfide exchange reactions have been extensively used for biomaterial modification, *e.g.*, with pyridyl disulfide derivatives of biopolymers having a labile pyridyl thiol to efficiently lead to hydrogel formation by disulfide crosslinking. The by-product of this reaction is pyridine-2-thione which is easily quantifiable by UV-spectroscopy, thus, the reaction conversion can be conveniently monitored. The thiol-disulfide exchange reaction has also been used to prepare a dual cross-linked self-healing hydrogel for bone regeneration with a bisphosphonate-modified HA.<sup>55</sup> Disulfide-crosslinked hydrogels are also developed by air oxidation of different thiol-modified polymers. Such a strategy leads to both intra and intermolecular crosslinks that remain dynamic. The disulfide crosslinked hydrogels have an advantage for cellular delivery applications as these bonds can be cleaved by endogenous enzymes such as glutathione which is released by cells over time enabling migration of cells within the biomaterial.<sup>56,57</sup> One limitation of such thiol-modified material for delivering therapeutic proteins is, as stated, the potential interaction of free thiols in the system with the tertiary structure of the encapsulated proteins, which could affect the *in vivo* outcome.<sup>51</sup>

### 2.4. Diels–Alder reaction

The Diels–Alder reaction is one of the reactions to form carbon–carbon bonds between molecules. It involves the reaction of a conjugated diene and a substituted alkene to form a six-membered cyclic structure.<sup>58</sup> The high atom efficiency and good regio-and stereoselectivity in the absence of catalyst



make this conjugation strategy suitable for several bioconjugation applications.<sup>58</sup> The Diels–Alder reaction is exothermic, therefore the products formed are stable as the retro Diels–Alder reaction is energetically demanding especially at room temperature.<sup>59</sup> However, when the reaction is carried out with electron-rich dienes and electron-poor dienophile reactants, for example, anthracene and tetracyanoethylene, the retro Diels–Alder reaction can take place at room temperature.<sup>60</sup> Furthermore, the equilibrium of reversible Diels–Alder reactions is not sensitive to water, which is a notable advantage for hydrogel preparation.<sup>61</sup> In a research study, Wei *et al.* synthesized a self-healing dextran hydrogel using a Diels–Alder reaction of fulvene-modified dextran and dichloromaleic acid-modified poly(ethylene glycol) (PEG) substrates and the gelation observed under physiological conditions.<sup>59</sup> Furan and maleimide are other predominantly used substrates for hydrogel preparation using a Diels–Alder reaction.<sup>62</sup> In this regard, an injectable biocompatible HA hydrogel prepared by mixing HA-furan and PEG-bismaleimide under physiological conditions which were utilized for intrathecal delivery of bioactive brain-derived neurotrophic factor to the injured spinal cord.<sup>63</sup> In subsequent studies, the HA-furan was replaced with the more electron-rich HA-methylfuran to enhance the cross-linking reaction at physiological pH.<sup>64</sup> The methyl-substituted furan lowers the free energy of the transition state as compared to the unsubstituted furan and leads to a 35-fold increase in the rate constant. The short gelation time at physiological pH and degradability at 37 °C makes it suitable for biomedical applications that require degradable linkages, such as for developing drug delivery systems or scaffolds for tissue engineering.

## 2.5. Boronic ester

The reaction between boronic acids and diols is efficient and reversible in an aqueous solution. By altering substrate structure, the hydrolytic stability of the resultant boronic esters can vary.<sup>65–67</sup> Boronic ester formation occurs at neutral pH, although it is more favorable at a high pH, where the boronate ion exists at a high concentration. Attributed to the rehybridization of boron from  $sp^2$  (boronic ester) to  $sp^3$  (boronate ester) and release of angle strain, the esters formed from hydroxyboronate species show higher hydrolytic stability than those formed from boronic ester.<sup>65,66</sup> The boronic esters are pH-sensitive and undergo hydrolysis at acidic pH.<sup>68</sup> Generally, acyclic boronic esters and small unhindered cyclic esters have rapid hydrolysis, while the hindered esters such as phenylboron pinacolate hydrolyze at a slower rate.<sup>65</sup> Boronic acid-containing hydrogels have significant potential in sensor design, controlled drug release, HIV-barrier, and 3D cell culture.<sup>69</sup> Heleg-Shabtai *et al.* designed a boronic acid-modified hydrogel for the controlled release of anticancer drug gossypol.<sup>68</sup> Here gossypol is used as a crosslinking agent that forms a boronate ester bond with phenylboronic acid-modified acrylamide copolymer chains leading to hydrogel formation. The gel is dissociated quickly in an acidic environment in the presence of lactic acid, which resembles the *in vivo* microenvironment of

cancer cells. This stimuli-responsive dissociation allows the controlled release of gossypol.<sup>69</sup> Phenylboronic acid-functionalized hydrogels were also investigated as optical glucose sensors for *in vivo* glucose monitoring systems.<sup>67</sup>

Boronic acid-containing hydrogels have self-healing properties due to the exchange between the boronic acid/diol and boronate esters. This exchange is most effective when the pH is near the  $pK_a$  value of boronic acids, which is usually around 8–9.<sup>66,69</sup> Recently, a boronic ester-crosslinked hydrogel was prepared from water-soluble diol-containing polymers and 2-acrylamidophenylboronic acid (2APBA) polymer. The intramolecular B–O coordination in 2APBA would promote boronic acid–diol complexation and provides the self-healing of the hydrogel at neutral and acidic pH, which were previously considered too low pH for boronic acid-containing materials.<sup>69</sup>

## 3. DCC HA nanoparticles

The cell surface receptors such as CD44 are overexpressed in cancer cells as compared to normal cells.<sup>70</sup> Due to the specific binding of HA to the CD44 receptor, HA-based nanoparticles are evaluated to develop targeted cancer treatment. HA nanoparticles have been reported to improve the delivery of small molecule drugs, nucleic acids, and proteins to CD44 positive cancer cells.<sup>71–73</sup> Although HA of moderate molecular weight above 100 kDa is considered more effective in binding CD44 receptors, liposomal formulations with low molecular weight HA (20–40 kDa) were shown to improve tumor specificity and reduce non-specific interactions as HA receptors that are ubiquitously expressed.<sup>74</sup> HA-based nanoparticles were widely synthesized either by inducing self-assembly with a chemical modification or together with cationic biopolymers and by coating HA on the nanoparticles. Anti-tumor drugs such as doxorubicin (DOX) which are lipophilic and less soluble in water were delivered specifically to CD44-positive cancer cells by self-assembled HA-based nanoparticles.<sup>75</sup> Dynamic covalent chemistry such as imine linkage, oxime linkage, hydrazone linkage, disulfide exchange, and boronic ester chemistry are also utilized to synthesize HA-based nanoparticles.<sup>76–79</sup>

As HA consists of glucuronic acid and *N*-acetyl glucosamine repeat units with abundant carboxylate and hydroxy groups, these functional groups were easily modified to develop bioactive nanomaterials and hydrogels.<sup>80</sup> The hydroxyls at the C2 and C3 positions of the glucuronic acid ring in HA can be oxidized using sodium periodate to produce two aldehyde groups per repeating unit of HA.<sup>81</sup> This method leads to partial degradation of the HA polymer chains. We have previously shown that the incorporation of aminoglycerol units on the HA backbone allows site-specific oxidation of incorporated diols within 5-minutes of periodate treatment leading to aldehyde formation without breaking the C2–C3 hydroxyls on HA.<sup>82</sup> Aldehyde-modified HA was also used to make pH-sensitive self-assemble nanoparticles by conjugating them to small molecule drugs and biopolymers through imine bond formation. Lei *et al.* utilized the sodium periodate oxidation of



HA and conjugated DOX and amino ferrocene (AFc) through a Schiff base reaction (Fig. 4a). DOX and AFc conjugated HA were self-assembled to form a pH-responsive drug-loaded HA-based nanoparticle. They also observed the release of DOX and AFc increases with a decrease in pH, which shows the more release of drugs in the tumor microenvironment through DCC bond cleavage.<sup>83</sup> Hu *et al.* modified the HA with benzaldehyde at multiple positions using covalent conjugation and used DOX to form a Schiff base dynamic covalent bond with benzaldehyde. DOX-loaded HA was self-assembled to form pH-sensitive nanoparticles.<sup>84</sup> Aldehyde-modified HA was also conjugated to DOX and cisplatin through imine bond formation

and chelation. These drug conjugates employing DCC were loaded into nanoparticles by electrostatic interactions with positively charged hydroxyethyl chitosan or chitosan using layer-by-layer self-assembly.<sup>85,86</sup> HA dialdehyde obtained by the periodate treatment forms an imine bond with chitosan leading to self-crosslinkable nanoparticles. Liang *et al.* used HA dialdehyde and chitosan nanoparticles to deliver the siRNA to treat bladder cancer.<sup>87</sup> Oxidized HA was also utilized to coat the nanoparticles with amine modification on their surfaces, *e.g.*, Liu *et al.* demonstrated the HA coating on amine-modified silica nanoparticles that encapsulated CuS for photothermal treatment.<sup>88</sup> Other examples include di-alde-

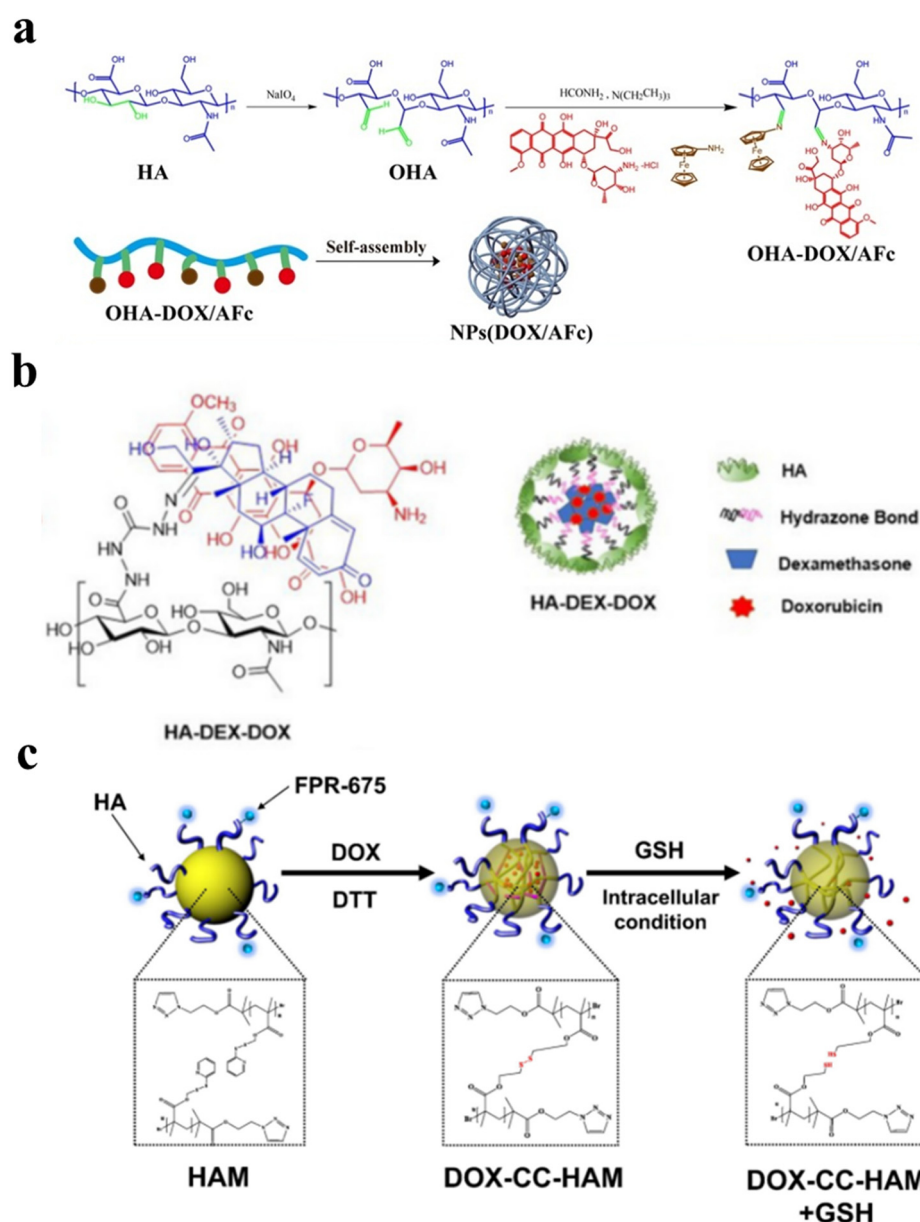


**Fig. 4** (a) Schematic representation of the synthetic process of OHA (oxidised hyaluronic acid)-DOX/AFc prodrugs and self-assembly of nanoparticles,<sup>83</sup> (b) the schematic illustration of the synthetic strategy for designing self-assembled HA-DEX-DOX nanoparticles,<sup>79</sup> and (c) the schematic representation of core-crosslinked hyaluronic acid polymeric micelles loaded with doxorubicin (DOX-CC-HAMs).<sup>92</sup>

hyde modified HA co-conjugated with DOX and dopamine using a Schiff base reaction by forming the imine bond. HA-DOX-dopamine (DAHA) conjugate was coated on chitosan-coated gold nanorods (GNR) by the layer-by-layer assembly. This nanoformulation was tested against breast cancer which showed both pH responsiveness due to the presence of an imine bond and a near-infrared (NIR) photothermal effect due to the presence of GNRs.<sup>89</sup>

Together with the Schiff base reaction, hydrazone bond formation is also used conventionally to form pH-sensitive nanoparticles. Our group recently reported the development of a self-assembled nanoparticle where dexamethasone (DEX) conjugated HA (hydrazone chemistry) was used as the hydrophobic moiety (Fig. 4b). We successfully loaded DOX into the HA-DEX nanoparticle (HA-DEX-DOX) by exploiting the hydrophobic interactions. Interestingly, the HA-DEX-DOX nanoparticle suppressed the DOX-induced platelet aggregation and thromboinflammation, in human whole blood.<sup>79</sup> Together with CDH, ADH was also used to functionalize the acid group in HA. Cai *et al.* modified the HA with ADH and used NHS/EDC coupling to conjugate deoxycholic acid (DOCA) to HA-ADH, which induced nanoparticle formation by self-assembly.<sup>71</sup> Similarly, hydrazone DCC chemistry was used to conjugate HA-ADH with curcumin (CUR). Curcumin is a small molecule with promising antitumor effects and is poorly soluble in water. The formation of HA-CUR conjugate through hydrazone linkage immediately induces the self-assembly of the polymeric conjugate in water.<sup>90</sup> Similar to CUR, other drugs having carbonyl groups such as DOX were conjugated with hydrazide functionalized HA through hydrazone linkage which also self-assemble to form nanoparticles due to the high hydrophobicity of DOX.<sup>91</sup> This acid labile pH-sensitive HA-DOX conjugate was more stable under physiological conditions as compared to the HA-DOX conjugates obtained by Schiff-base chemistry.

Nanoparticles obtained employing disulfide exchange reactions have been developed to harness the excess availability of glutathione, a disulfide reducing agent, in cancer cells as compared to healthy tissue. The disulfide bond is stable to pH and water and can be only reduced in the presence of other thiols such as glutathione. Han *et al.* synthesized a bio-reducible disulfide core-based HA micelle (Fig. 4c). They opened the reducing end of HA and modified the C1 carbon with an alkyne moiety. Disulfide-containing azide linker was synthesized to conjugate with HA-alkyne through Huisgen cycloaddition. HA-disulfide forms a crosslink at the core of the micelle that allows intracellular disassembly of the nanoparticle by a thiol exchange reaction. DOX was loaded into HA-disulfide micelle with high loading efficiency (>80%) that was demonstrated to effectively deliver DOX to cancer cells.<sup>92</sup> Similarly, Han *et al.* used Huisgen cycloaddition to conjugate HA with polycaprolactone. In this strategy, the carboxyl group of HA was first modified with a pyridyl disulfide reagent using NHS/EDC (*N*-hydroxysuccinimide/1-ethyl-3-(3-dimethylaminopropyl) carbodiimide hydrochloride) coupling chemistry, followed by the incorporation of polycaprolactone to form nanoparticles.

The cleavage of pyridyl disulfide groups resulted in the formation of disulfide-crosslinked HA-based nanoparticles.<sup>93</sup> Other strategies have also been developed to obtain disulfide-modified HA nanoparticles. This includes conjugation of cystamine using the traditional carbodiimide method that was used as a functional handle to incorporate other hydrophobic groups such as docosahexaenoic acid (DHA) and chlorin e6 (Ce6), which induced self-assembly.<sup>94</sup> Cystamine was also conjugated at the reducing-end of HA that was later conjugated to the NHS modified albumin to give HA-cystamine-albumin conjugate that formed micelle-like nanoparticles.<sup>95</sup> Similarly, alkyne moiety was incorporated at the reducing end of HA that was used to conjugate poly trimethylene carbonate-*co*-dithiolane trimethylene carbonate (P(TMC-*co*-DTC) by click chemistry that yielded self-assembled nanoparticle formation. These nanoparticles allowed efficient loading of thiol-containing drugs such as mertansine through disulfide-exchange reactions.<sup>96</sup> A similar strategy was used to obtain HA conjugated poly-D,L-lactide (PDLLA) that formed self-assembled nanoparticles when mixed with star PLGA having a five-membered disulfide ring at the terminal end. The HA-star PLGA nanoparticle was crosslinked at the core using dithiothreitol (DTT) and loaded with docetaxel (DTX). These nanoparticles with redox-sensitive groups showed less toxicity as compared to the DTX-HA-PLGA nanoparticle without any disulfide crosslinks.<sup>77</sup>

Collectively with imine and hydrazone chemistry, boronic ester DCC are also pH-responsive bonds that are less stable under acidic pH conditions. Arylboronic esters were widely used in biomedical applications due to the disintegration of the boronic ester bonds in the presence of oxygen and reactive oxygen species (ROS). Chen *et al.* synthesized the arylboronic ester functionalized HA having a cholesterol moiety which resulted in self-assembled nanoparticle formation. Indocyanine green (ICG) and DOX were loaded into the nanoparticle for the combination of photothermal therapy and chemotherapy. Irradiation of this nanoparticle using 808 nm NIR laser-induced the production of ROS which disintegrated the arylboronic ester releasing the loaded DOX.<sup>97</sup> Other arylboronic acid derivatives were also developed such as by conjugating 3-aminophenyl boronic acid (APBA) that was cross-linked with tannic acid through catechol-boronate complexation to yield nanoparticles. pH-responsive<sup>98</sup> The phenyl boronic acid derivative of HA was also used to conjugate cyclodextrin to enable the encapsulation of small molecule drugs such as PTX. To obtain nanoparticles, these modified polymers were coated with polydopamine nanoparticles. Conjugation of other targeting ligands such as triphenylphosphonium (TPP) enabled dual targeting of these nanoparticles (CD44 targeting *via* HA and mitochondria targeting *via* TPP).<sup>99</sup> Boronic acid interaction with cell-surface sialic acid was also utilized to improve cell-specific targeting as demonstrated using APBA conjugated HA-ceramic (HACE) based nanoparticles.<sup>100</sup> Additionally, the comprehensive research focused on DCC crosslinked HA-based nanoparticles, the type of DCC bond, and the applications of these nanoparticles are summarized in Table 2.



**Table 2** HA-based nanoparticles using DCC chemistry

No.	DCC type	Application	Reference
1	Schiff base	siRNA delivery to treat bladder cancer	Liang <i>et al.</i> <sup>142</sup>
2	Schiff base	Synergic chemotherapy and photodynamic therapy of breast cancer	Y. Wang, Qian, <i>et al.</i> <sup>86</sup>
3	Schiff base	Chemo-photothermal synergic therapy of atherosclerosis	Y. Wang, Yang, <i>et al.</i> <sup>143</sup>
4	Schiff base	pH-Sensitive nanoparticles for antitumor applications	S. Liu <i>et al.</i> <sup>88</sup>
5	Schiff base	NIR/pH dual responsive materials for synergic chemo-photothermal therapy	X. Zhang <i>et al.</i> <sup>78</sup>
6	Schiff base	pH-Sensitive drug delivery for combined chemotherapy and chemo dynamic therapy	W. Xu <i>et al.</i> <sup>89</sup>
7	Schiff base	HA-coated silica nanoparticles for chemo – photodynamic combination therapy	Lei <i>et al.</i> <sup>83</sup>
8	Schiff base	HA-coated nanoparticles for combined photothermal and gene therapy.	K. Chen <i>et al.</i> <sup>144</sup>
9	Schiff base and disulfide bond	HA coated nanoparticles for pH and redox sensitive drug delivery systems.	Yanjun Liu <i>et al.</i> <sup>145</sup>
10	Schiff base	HA-based nanoparticles with aggregation induced emission.	Shao <i>et al.</i> <sup>146</sup>
11	Hydrazone bond	Anti-tumor targeted drug delivery	D. Wei <i>et al.</i> <sup>147</sup>
12	Hydrazone bond	pH-Responsive HA-based nanoparticles for enhanced cancer therapy and targeted curcumin delivery	Cai <i>et al.</i> <sup>71</sup>
13	Hydrazone bond	HA-based nanoparticles for combination therapy by suppressing inflammation and promoting antitumor macrophage polarization	Lai <i>et al.</i> <sup>90</sup>
14	Hydrazone bond	HA-based nanoparticles for enhanced delivery of DOX	Rangasami <i>et al.</i> <sup>79</sup>
15	Hydrazone and disulfide bonds	Redox and pH dual sensitive HA nanoparticles for targeted DOX delivery	Liao <i>et al.</i> <sup>91</sup>
16	Hydrazone bond	Enzyme and pH-responsive HA-based nanoparticles with synergic chemotherapy and photodynamic therapy.	M. Xu <i>et al.</i> <sup>148</sup>
17	Hydrazone bond	HA coated nanoparticles for non-small cell lung cancer combination therapy.	Ren <i>et al.</i> <sup>149</sup>
18	Disulfide bond	Targeted and triggered release of DTX in the tumor reducing environments	Pang <i>et al.</i> <sup>150</sup>
19	Disulfide bond	High drug encapsulation of HA shelled disulfide crosslinked nanoparticles	X. Wang <i>et al.</i> <sup>77</sup>
20	Disulfide bond	HA/albumin micelle like nanoparticles for delivery of DOX	Yue Zhang <i>et al.</i> <sup>96</sup>
21	Disulfide bond	Disulfide cross linked HA nanoparticles for targeted tumor therapy	Curcio <i>et al.</i> <sup>95</sup>
22	Disulfide bond	Disulfide core-crosslinked HA micelle for targeted cancer therapy	H. S. Han, Thambi, <i>et al.</i> <sup>93</sup>
23	Disulfide bond	PTX loaded redox sensitive HA-based nanoparticles to treat lung cancer.	H. S. Han, Choi, <i>et al.</i> <sup>92</sup>
24	Disulfide bond	Redox sensitive HA-based self-assemble nanoparticles for targeted cancer therapy	Song <i>et al.</i> <sup>151</sup>
25	Disulfide bond	GSH sensitive HA-based micelles for intracellular delivery of DOX to colon cancer cells and cancer stem cells.	Lu <i>et al.</i> <sup>152</sup>
26	Disulfide bond	Redox sensitive HA – poly-L-histidine copolymer for treating tumor	Debele <i>et al.</i> <sup>153</sup>
27	Disulfide bond	Reduction sensitive HA-based prodrug micelles for targeting tumor.	Lee <i>et al.</i> <sup>154</sup>
28	Disulfide bond	Redox-responsive HA-based nanoparticles for synergic chemotherapy and photodynamic therapy against breast cancer	M. Li <i>et al.</i> <sup>155</sup>
29	Boronic ester	NIR light triggered pH-sensitive nanoparticles for dual chemo-photodynamic therapy	Wang <i>et al.</i> <sup>94</sup>
30	Boronic ester	HA-tannic acid nanoparticles as a smart antibacterial system	Y. Chen <i>et al.</i> <sup>97</sup>
31	Boronic ester	pH-Responsive HA-coated fluorescent nanoparticles for intracellular delivery	Montanari <i>et al.</i> <sup>98</sup>
32	Boronic ester	pH-Sensitive self-assembling HA-based nanoparticles for tumor targeting and penetration.	S. H. Kim <i>et al.</i> <sup>99</sup>
33	Boronic ester and disulfide bond	Redox and pH dual sensitive HA-based nanoparticles for targeting glioma.	Jeong <i>et al.</i> <sup>100</sup>
34	Boronic ester	HA-coated silica nanoparticles for synergic chemo-photodynamic therapy	M. Zhang <i>et al.</i> <sup>76</sup>
35	Boronic ester	BODIPY conjugates HA-based nanoparticles for dual photodynamic and photothermal therapy.	Zhou <i>et al.</i> <sup>156</sup>
36	Boronic ester	Radio sensitive HA-based nanoparticle for radioprotection	B. Chen <i>et al.</i> <sup>157</sup>

## 4. Conclusion

Different crosslinking chemistries to develop HA-based hydrogels and nanomaterials have been pursued by several research groups, including physical and chemical crosslinking methods. However, DCC remains one of the most promising methods to obtain materials that allow a catalyst-free crosslinking strategy with high specificity and without any toxic by-products. It should be noted that HA is not an inert molecule and therefore different chemical modifications can change its biological properties that could augment or limit its biological effects. For example, if the scientific aim is to develop

materials to deliver sensitive proteins, one should avoid using chemical modifications with high thiol contents (affects their tertiary structure).<sup>51</sup> On the other hand, the modifications that stabilize the proteins, similar to the natural ECM could augment the biological outcome.<sup>23</sup> Such design principles are also important to develop nanomaterials. Specific incorporation of hydrophobic residues or chemical modifications such as disulfide bonds could stabilize small molecule drugs and promote intracellular trafficking of biologics. Because of the dynamic nature of the covalent bonds in DCC, such chemical reactions are best suited for stimuli-responsive drug release. Employing HA to develop such biomaterials not only improves

the biocompatibility of the drug carrier but also allows targeted delivery of the cargo molecules. Thus, HA-based hydrogels and nanomaterials have shown considerable potential in several bio-related areas, such as drug delivery, tissue regeneration, sensors, gene transfection, and other biomedical applications.

## Conflicts of interest

There are no conflicts to declare.

## Acknowledgements

Financial assistance for this review was provided by the Swedish Strategic Research 'StemTherapy' (Dnr 2009-1035), the Swedish Research Council (Dnr 2020-04025), European Union's EUREKA/Eurostars-2 (nr. 2020-03601), and European Union's Horizon 2020 Marie Skłodowska-Curie H2020-MSCA-ITN-ETN-2020 (nr. 955335).

## Notes and references

- 1 A. D. Theocharis, S. S. Skandalis, C. Gialeli and N. K. Karamanos, *Adv. Drug Delivery Rev.*, 2015, **1**, 4–27.
- 2 K. KA and A. KS, *Ann. Biomed. Eng.*, 2015, **43**, 489–500.
- 3 E. Papakonstantinou, M. Roth and G. Karakiulakis, *Derm.-Endocrinol.*, 2012, **4**, 253.
- 4 R. C. Gupta, R. Lall, A. Srivastava and A. Sinha, *Front. Vet. Sci.*, 2019, **6**, 192.
- 5 G. Kogan, L. Šoltés, R. Stern and P. Gemeiner, *Biotechnol. Lett.*, 2007, **29**, 17–25.
- 6 M. Dovedyti, Z. J. Liu and S. Bartlett, *Eng. Regener.*, 2020, **1**, 102–113.
- 7 A. Avenoso, A. D'Ascola, M. Scuruchi, G. Mandraffino, A. Calatroni, A. Saitta, S. Campo and G. M. Campo, *Inflammation Res.*, 2018, **67**, 5–20.
- 8 C. E. Schanté, G. Zuber, C. Herlin and T. F. Vandamme, *Carbohydr. Polym.*, 2011, **85**, 469–489.
- 9 M. Litwiniuk, A. Krejner-Bienias, A. R. Gauto and T. Grzela, *Wounds*, 2016, **28**, 78–88.
- 10 M. P. Paidikondala, V. K. Rangasami, G. N. Nawale, T. Casalini, G. Perale, S. Kadekar, G. Mohanty, T. Salminen and O. P. Oommen, *Angew. Chem., Int. Ed.*, 2019, **58**, 2815–2819.
- 11 S. Khunmanee, Y. Jeong and H. Park, *J. Tissue Eng.*, 2017, **8**, DOI: [10.1177/2041731417726464](https://doi.org/10.1177/2041731417726464).
- 12 L. A. Pérez, R. Hernández, J. M. Alonso, R. Pérez-González and V. Sáez-Martínez, *Biomedicines*, 2021, **9**, 1113.
- 13 J. Faivre, A. I. Pigweh, J. Iehl, P. Maffert, P. Gockjian and F. Bourdon, *Expert Rev. Med. Devices*, 2021, **12**, 1175–1187.
- 14 Q. Huang, Y. Zou, M. C. Arno, S. Chen, T. Wang, J. Gao, A. P. Dove and J. Du, *Chem. Soc. Rev.*, 2017, **46**, 6255–6275.
- 15 J. M. Whitelock and R. V. Iozzo, *Chem. Rev.*, 2005, **105**, 2745–2764.
- 16 M. R. Arkenberg, H. D. Nguyen and C.-C. Lin, *J. Mater. Chem. B*, 2020, **8**, 7835–7855.
- 17 Y. Jin, C. Yu, R. J. Denman and W. Zhang, *Chem. Soc. Rev.*, 2013, **42**, 6634–6654.
- 18 M. Rizwan, A. E. G. G. Baker and M. S. Shoichet, *Adv. Healthcare Mater.*, 2021, **2100234**, 2100234.
- 19 M. M. Perera and N. Ayres, *Polym. Chem.*, 2020, **11**, 1410–1423.
- 20 Y. Liu and S. Hsu, *Front. Chem.*, 2018, 449.
- 21 S. Tavakoli and A. S. Klar, *Biomolecules*, 2020, **10**, 1169.
- 22 S. Hinderer, L. S. Layland and K. Schenke-Layland, *Adv. Drug Deliv. Rev.*, 2016, **97**, 260–269.
- 23 H. J. Yan, T. Casalini, G. Hulsart-Billström, S. Wang, O. P. Oommen, M. Salvalaglio, S. Larsson, J. Hilborn and O. P. Varghese, *Biomaterials*, 2018, **161**, 190–202.
- 24 C. B. Highley, G. D. Prestwich and J. A. Burdick, *Curr. Opin. Biotechnol.*, 2016, **40**, 35–40.
- 25 H. Wang, S. C. Heilshorn, H. Wang and S. C. Heilshorn, *Adv. Mater.*, 2015, **27**, 3717–3736.
- 26 M. Tanaka, M. Nakahata, P. Linke and S. Kaufmann, *Polym. J.*, 2020, **52**, 861–870.
- 27 S. Tang, B. M. Richardson and K. S. Anseth, *Prog. Mater. Sci.*, 2021, **120**, 100738.
- 28 E. H. Cordes and W. P. Jencks, *J. Am. Chem. Soc.*, 1962, **84**, 832–837.
- 29 W. P. Jencks, *J. Am. Chem. Soc.*, 1959, **81**, 475–481.
- 30 D. Bermejo-Velasco, A. Azémard, O. P. Oommen, J. Hilborn and O. P. Varghese, *Biomacromolecules*, 2019, **20**, 1412–1420.
- 31 C. Y. Lin, H. H. Peng, M. H. Chen, J. S. Sun, T. Y. Liu and M. H. Chen, *J. Mater. Sci. Mater. Med.*, 2015, **26**, 1–12.
- 32 Y. Deng, J. Ren, G. Chen, G. Li, X. Wu, G. Wang, G. Gu and J. Li, *Sci. Rep.*, 2017, **7**, 1–13.
- 33 C. D. Spicer, *Polym. Chem.*, 2020, **11**, 184–219.
- 34 B. V. Slaughter, S. S. Khurshid, O. Z. Fisher, A. Khademhosseini and N. A. Peppas, *Adv. Mater.*, 2009, **21**, 3307–3329.
- 35 D. K. Kölmel and E. T. Kool, *Chem. Rev.*, 2017, **117**, 10358–10376.
- 36 J. Kalia and R. T. Raines, *Angew. Chem., Int. Ed.*, 2008, **47**, 7523–7526.
- 37 O. P. Oommen, S. Wang, M. Kisiel, M. Sloff, J. Hilborn and O. P. Varghese, *Adv. Funct. Mater.*, 2013, **23**, 1273–1280.
- 38 W. P. Jencks, *J. Am. Chem. Soc.*, 2002, **81**, 475–481.
- 39 S. Wang, G. N. Nawale, S. Kadekar, O. P. Oommen, N. K. Jena, S. Chakraborty, J. Hilborn and O. P. Varghese, *Sci. Rep.*, 2018, **8**, 1–7.
- 40 F. Saito, H. Noda and J. W. Bode, *ACS Chem. Biol.*, 2015, **10**, 1026–1033.
- 41 E. T. Kool, D. H. Park and P. Crisalli, *J. Am. Chem. Soc.*, 2013, **135**, 17663–17666.
- 42 A. Bandyopadhyay and J. Gao, *Chemistry*, 2015, **21**, 14748–14752.
- 43 D. D. McKinnon, D. W. Domaille, J. N. Cha and K. S. Anseth, *Chem. Mater.*, 2014, **26**, 2382–2387.

44 A. Dirksen, T. M. Hackeng, P. E. Dawson, A. Dirksen, P. E. Dawson, A. Dirksen and T. M. Hackeng, *Angew. Chem., Int. Ed.*, 2006, **45**, 7581–7584.

45 F. Trausel, C. Maity, J. M. Poolman, D. S. J. Kouwenberg, F. Versluis, J. H. Van Esch and R. Eelkema, *Nat. Commun.*, 2017, **8**, 1–7.

46 P. Crisalli and E. T. Kool, *J. Org. Chem.*, 2013, **78**, 1184–1189.

47 M. Wendeler, L. Grinberg, X. Wang, P. E. Dawson and M. Baca, *Bioconjugate Chem.*, 2014, **25**, 93–101.

48 P. Crisalli and E. T. Kool, *Org. Lett.*, 2013, **15**, 1646–1649.

49 J. Lou, F. Liu, C. D. Lindsay, O. Chaudhuri, S. C. Heilshorn and Y. Xia, *Adv. Mater.*, 2018, **30**, 1705215.

50 S. Wang, G. N. Nawale, O. P. Oommen, J. Hilborn and O. P. Varghese, *Polym. Chem.*, 2019, **10**, 4322–4327.

51 M. Paidikondala, S. Wang, J. Hilborn, S. Larsson and O. P. Varghese, *ACS Appl. Bio Mater.*, 2019, **2**, 2006–2012.

52 S. Samanta, L. Ylä-Outinen, V. K. Rangasami, S. Narkilahti and O. P. Oommen, *Acta Biomater.*, 2022, **140**, 314–323.

53 S. Samanta, V. K. Rangasami, H. Sarlus, J. R. K. Samal, A. D. Evans, V. S. Parihar, O. P. Varghese, R. A. Harris and O. P. Oommen, *Acta Biomater.*, 2022, **142**, 36–48.

54 W. R. Algar, *Chemosel. Bioorthogonal Ligation React.*, 2017, 1–36.

55 L. Shi, F. Wang, W. Zhu, Z. Xu, S. Fuchs, J. Hilborn, L. Zhu, Q. Ma, Y. Wang, X. Weng and D. A. Ossipov, *Adv. Funct. Mater.*, 2017, **27**, 1700591.

56 X. Z. Shu, Y. Liu, Y. Luo, M. C. Roberts and G. D. Prestwich, *Biomacromolecules*, 2002, **3**, 1304–1311.

57 C. S. Sevier and C. A. Kaiser, *Nat. Rev. Mol. Cell Biol.*, 2002, **3**, 836–847.

58 M. A. Tasdelen, *Polym. Chem.*, 2011, **2**, 2133–2145.

59 Z. Wei, J. H. Yang, X. J. Du, F. Xu, M. Zrinyi, Y. Osada, F. Li and Y. M. Chen, *Macromol. Rapid Commun.*, 2013, **34**, 1464–1470.

60 B. Masci, S. Pasquale and P. Thuéry, *Org. Lett.*, 2008, **10**, 4835–4838.

61 R. C. Boutelle and B. H. Northrop, *J. Org. Chem.*, 2011, **76**, 7994–8002.

62 M. Gregoritza and F. P. Brandl, *Eur. J. Pharm. Biopharm.*, 2015, **97**, 438–453.

63 T. Führmann, J. Obermeyer, C. H. Tator and M. S. Shoichet, *Methods*, 2015, **84**, 60–69.

64 L. J. Smith, S. M. Taimoori, R. Y. Tam, A. E. G. Baker, N. Binth Mohammad, J. F. Trant and M. S. Shoichet, *Biomacromolecules*, 2018, **19**, 926–935.

65 R. Lever and C. P. Page, *Nat. Rev. Drug Discovery*, 2002, **1**, 140–148.

66 W. L. A. Brooks and B. S. Sumerlin, *Chem. Rev.*, 2015, **116**, 1375–1397.

67 A. K. Yetisen, N. Jiang, A. Fallahi, Y. Montelongo, G. U. Ruiz-Esparza, A. Tamayol, Y. S. Zhang, I. Mahmood, S. A. Yang, K. S. Kim, H. Butt, A. Khademhosseini and S. H. Yun, *Adv. Mater.*, 2017, **29**, 1606380.

68 V. Heleg-Shabtai, R. Aizen, R. Orbach, M. A. Aleman-Garcia and I. Willner, *Langmuir*, 2015, **31**, 2237–2242.

69 Y. Guan and Y. Zhang, *Chem. Soc. Rev.*, 2013, **42**, 8106–8121.

70 S. C. Ghosh, S. Neslihan Alpay and J. Klostergaard, *Expert Opin. Ther. Targets*, 2012, **16**, 635–650.

71 J. Cai, J. Fu, R. Li, F. Zhang, G. Ling and P. Zhang, *Carbohydr. Polym.*, 2019, **208**, 356–364.

72 G. Jiang, K. Park, J. Kim, K. S. Kim, E. J. Oh, H. Kang, S. E. Han, Y. K. Oh, T. G. Park and S. K. Hahn, *Biopolymers*, 2008, **89**, 635–642.

73 E. Chiesa, A. Greco, F. Riva, R. Dorati, B. Conti, T. Modena and I. Genta, *Pharmaceutics*, 2021, **13**, 1565.

74 S. Mizrahy, S. R. Raz, M. Hasgaard, H. Liu, N. Soffer-Tsur, K. Cohen, R. Dvash, D. Landsman-Milo, M. G. E. G. Bremer, S. M. Moghimi and D. Peer, *J. Controlled Release*, 2011, **156**, 231–238.

75 Y. Chi, X. Yin, K. Sun, S. Feng, J. Liu, D. Chen, C. Guo and Z. Wu, *J. Controlled Release*, 2017, **261**, 113–125.

76 M. Zhang, S. Asghar, C. Tian, Z. Hu, Q. Ping, Z. Chen, F. Shao and Y. Xiao, *Carbohydr. Polym.*, 2021, **253**, 117194.

77 X. Wang, R. Cheng and Z. Zhong, *Acta Biomater.*, 2021, **125**, 280–289.

78 X. Zhang, D. Li, J. Huang, K. Ou, B. Yan, F. Shi, J. Zhang, J. Zhang, J. Pang, Y. Kang and J. Wu, *J. Mater. Chem. B*, 2019, **7**, 251–264.

79 V. K. Rangasami, S. Samanta, V. S. Parihar, K. Asawa, K. Zhu, O. P. Varghese, Y. Teramura, B. Nilsson, J. Hilborn, R. A. Harris and O. P. Oommen, *Carbohydr. Polym.*, 2021, **254**, 117291.

80 M. N. Collins, *Hyaluronic acid for Biomedical and Pharmaceutical Applications*, Smithers Rapra Technology, 2014.

81 K. A. Kristiansen, A. Potthast and B. E. Christensen, *Carbohydr. Res.*, 2010, **345**, 1264–1271.

82 S. Wang, O. P. Oommen, H. Yan and O. P. Varghese, *Biomacromolecules*, 2013, **14**, 2427–2432.

83 M. Lei, G. Chen, M. Zhang, J. Lei, T. Li, D. Li and H. Zheng, *Colloids Surf. B*, 2021, **203**, 111750.

84 R. Hu, H. Zheng, J. Cao, Z. Davoudi and Q. Wang, *J. Biomed. Nanotechnol.*, 2017, **13**, 1058–1068.

85 G. Lalevée, G. Sudre, A. Montembault, J. Meadows, S. Malaise, A. Crépet, L. David and T. Delair, *Carbohydr. Polym.*, 2016, **154**, 86–95.

86 Y. Wang, J. Qian, M. Yang, W. Xu, J. Wang, G. Hou, L. Ji and A. Suo, *Carbohydr. Polym.*, 2019, **225**, 115206.

87 Y. Liang, Y. Wang, L. Wang, Z. Liang, D. Li, X. Xu, Y. Chen, X. Yang, H. Zhang and H. Niu, *Bioact. Mater.*, 2021, **6**, 433.

88 S. Liu, Y. Zhao, M. Shen, Y. Hao, X. Wu, Y. Yao, Y. Li and Q. Yang, *J. Mater. Chem. B*, 2022, **10**, 562–570.

89 W. Xu, J. Wang, J. Qian, G. Hou, Y. Wang, L. Ji and A. Suo, *Mater. Sci. Eng., C*, 2019, **103**, 109854.

90 H. Lai, X. Ding, J. Ye, J. Deng and S. Cui, *Colloids Surf. B*, 2021, **198**, 111455.

91 J. Liao, H. Zheng, Z. Fei, B. Lu, H. Zheng, D. Li, X. Xiong and Y. Yi, *Int. J. Biol. Macromol.*, 2018, **113**, 737–747.



92 H. S. Han, K. Y. Choi, H. Ko, J. Jeon, G. Saravanakumar, Y. D. Suh, D. S. Lee and J. H. Park, *J. Controlled Release*, 2015, **200**, 158–166.

93 H. S. Han, T. Thambi, K. Y. Choi, S. Son, H. Ko, M. C. Lee, D. G. Jo, Y. S. Chae, Y. M. Kang, J. Y. Lee and J. H. Park, *Biomacromolecules*, 2015, **16**, 447–456.

94 R. Wang, H. Yang, A. R. Khan, X. Yang, J. Xu, J. Ji and G. Zhai, *J. Colloid Interface Sci.*, 2021, **598**, 213–228.

95 M. Curcio, L. Diaz-Gomez, G. Cirillo, F. P. Nicoletta, A. Leggio and F. Iemma, *Pharmaceutics*, 2021, **13**, 1–16.

96 Y. Zhang, K. Wu, H. Sun, J. Zhang, J. Yuan and Z. Zhong, *ACS Appl. Mater. Interfaces*, 2018, **10**, 1597–1604.

97 Y. Chen, H. Li, Y. Deng, H. Sun, X. Ke and T. Ci, *Acta Biomater.*, 2017, **51**, 374–392.

98 E. Montanari, A. Gennari, M. Pelliccia, C. Gourmet, E. Lallana, P. Matricardi, A. J. McBain and N. Tirelli, *Macromol. Biosci.*, 2016, **16**, 1815–1823.

99 S. H. Kim, I. In and S. Y. Park, *Biomacromolecules*, 2017, **18**, 1825–1835.

100 J. Y. Jeong, E. H. Hong, S. Y. Lee, J. Y. Lee, J. H. Song, S. H. Ko, J. S. Shim, S. Choe, D. D. Kim, H. J. Ko and H. J. Cho, *Acta Biomater.*, 2017, **53**, 414–426.

101 C. Han, H. Zhang, Y. Wu, X. He and X. Chen, *Sci. Rep.*, 2020, **10**, 14997.

102 S. Li, M. Pei, T. Wan, H. Yang, S. Gu, Y. Tao, X. Liu, Y. Zhou, W. Xu and P. Xiao, *Carbohydr. Polym.*, 2020, **250**, 116922.

103 C. Qian, T. Zhang, J. Gravesande, C. Baysah, X. Song and J. Xing, *Int. J. Biol. Macromol.*, 2019, **123**, 140–148.

104 S. W. Kim, D. Y. Kim, H. H. Roh, H. S. Kim, J. W. Lee and K. Y. Lee, *Biomacromolecules*, 2019, **20**, 1860–1866.

105 X. Ma, X. Liu, P. Wang, X. Wang, R. Yang, S. Liu, Z. Ye and B. Chi, *ACS Appl. Bio Mater.*, 2020, **3**, 4036–4043.

106 W. Kong, Y. Gao, Q. Liu, L. Dong, L. Guo, H. Fan, Y. Fan and X. Zhang, *Int. J. Biol. Macromol.*, 2020, **160**, 1201–1211.

107 J. Sun, C. Xiao, H. Tan and X. Hu, *J. Appl. Polym. Sci.*, 2013, **129**, 682–688.

108 H. Tan, H. Li, J. P. Rubin and K. G. Marra, *J. Tissue Eng. Regener. Med.*, 2011, **5**, 790–797.

109 M. Weis, J. Shan, M. Kuhlmann, T. Jungst, J. Tessmar and J. Groll, *Gels*, 2018, **4**, 82.

110 H. Tan, C. R. Chu, K. A. Payne and K. G. Marra, *Biomaterials*, 2009, **30**, 2499–2506.

111 T. Hozumi, T. Kageyama, S. Ohta, J. Fukuda and T. Ito, *Biomacromolecules*, 2018, **19**, 288–297.

112 Z. Li, L. Liu and Y. Chen, *Acta Biomater.*, 2020, **110**, 119–128.

113 H. Wang, D. Zhu, A. Paul, L. Cai, A. Enejder, F. Yang and S. C. Heilshorn, *Adv. Funct. Mater.*, 2017, **27**, 1605609.

114 D. Zhu, H. Wang, P. Trinh, S. C. Heilshorn and F. Yang, *Biomaterials*, 2017, **127**, 132–140.

115 L. L. Wang, C. B. Highley, Y.-C. Yeh, J. H. Galarraga, S. Uman and J. A. Burdick, *J. Biomed. Mater. Res., Part A*, 2018, **106**, 865–875.

116 F. Chen, Y. Ni, B. Liu, T. Zhou, C. Yu, Y. Su, X. Zhu, X. Yu and Y. Zhou, *Carbohydr. Polym.*, 2017, **166**, 31–44.

117 Z. Li, F. Zhou, Z. Li, S. Lin, L. Chen, L. Liu and Y. Chen, *ACS Appl. Mater. Interfaces*, 2018, **10**, 25194–25202.

118 G. Janarthanan, H. S. Shin, I.-G. Kim, P. Ji, E.-J. Chung, C. Lee and I. Noh, *Biofabrication*, 2020, **12**, 045026.

119 V. G. Muir, T. H. Qazi, S. Weintraub, B. O. Torres Maldonado, P. E. Arratia and J. A. Burdick, *Small*, 2022, **18**, 2201115.

120 A. G. Baker, R. Y. Tam and M. J. Shoichet, *Biomacromolecules*, 2017, **18**, 4373–4384.

121 M. H. Asim, S. Silberhumer, I. Shahzadi, A. Jalil, B. Matusczak and A. Bernkop-Schnürch, *Carbohydr. Polym.*, 2020, **237**, 116092.

122 J. L. Young, J. Tuler, R. Braden, P. Schüp-Magoffin, J. Schaefer, K. Kretschmer, K. L. Christman and A. J. Engler, *Acta Biomater.*, 2013, **9**, 7151–7157.

123 A. Skardal, J. Zhang, L. McCoard, S. Oottamasathien and G. D. Prestwich, *Adv. Mater.*, 2010, **22**, 4736–4740.

124 S. Bian, M. He, J. Sui, H. Cai, Y. Sun, J. Liang, Y. Fan and X. Zhang, *Colloids Surf., B*, 2016, **140**, 392–402.

125 L. Wu, S. D. Cio, H. S. Azevedo and J. E. Gautrot, *Biomacromolecules*, 2020, **21**, 4663–4672.

126 W. Cao, J. Sui, M. Ma, Y. Xu, W. Lin, Y. Chen, Y. Man, Y. Sun, Y. Fan and X. Zhang, *J. Mater. Chem. B*, 2019, **7**, 4413–4423.

127 Y. Zhang, X. Li, N. Zhong, Y. Huang, K. He and X. Ye, *J. Biomat. Sci.*, 2019, **30**, 995–1007.

128 S. Deng, X. Li, W. Yang, K. He and X. Ye, *J. Biomat. Sci.*, 2018, **29**, 1643–1655.

129 S.-Y. Choh, D. Cross and C. Wang, *Biomacromolecules*, 2011, **12**, 1126–1136.

130 A. Sigen, Q. Xu, M. Johnson, J. Creagh-Flynn, M. Venet, D. Zhou, I. Lara-Sáez, H. Tai and W. Wang, *Appl. Mater. Today*, 2021, **22**, 100967.

131 C. Yu, H. Gao, Q. Li and X. Cao, *Polym. Chem.*, 2020, **11**, 3169–3178.

132 F. Yu, X. Cao, J. Du, G. Wang and X. Chen, *ACS Appl. Mater. Interfaces*, 2015, **7**, 24023–24031.

133 F. Yu, X. Cao, Y. Li, L. Zeng, B. Yuan and X. Chen, *Polym. Chem.*, 2013, **5**, 1082–1090.

134 X. Hu, Z. Gao, H. Tan, H. Wang, X. Mao and J. Pang, *Front. Chem.*, 2019, 477.

135 G. Wang, X. Cao, H. Dong, L. Zeng, C. Yu and X. Chen, *Polymers*, 2018, **10**, 949.

136 V. Delplace, P. E. B. Nickerson, A. Ortin-Martinez, A. E. G. Baker, V. A. Wallace and M. S. Shoichet, *Adv. Funct. Mater.*, 2020, **30**, 1903978.

137 T. Figueiredo, Y. Ogawa, J. Jing, V. Cosenza, I. Jeacomine, J. D. M. Olsson, T. Gerfaud, J. G. Boiteau, C. Harris and R. Auzély-Velty, *Polym. Chem.*, 2020, **11**, 3800–3811.

138 W. Shi, B. Hass, M. A. Kuss, H. Zhang, S. Ryu, D. Zhang, T. Li, Y. Li and B. Duan, *Carbohydr. Polym.*, 2020, **233**, 115803.

139 M. M. D. Oliveira, C. V. Nakamura and R. Auzély-Velty, *Carbohydr. Polym.*, 2020, **247**, 116845.

140 T. Figueiredo, J. Jing, I. Jeacomine, J. Olsson, T. Gerfaud, J.-G. Boiteau, C. Rome, C. Harris and R. Auzély-Velty, *Biomacromolecules*, 2019, **21**, 230–239.

141 D. Tarus, E. Hachet, L. Messager, B. Catargi, V. Ravaine and R. Auzély-Velty, *Macromol. Rapid Commun.*, 2014, **35**, 2089–2095.

142 Y. Liang, Y. Wang, L. Wang, Z. Liang, D. Li, X. Xu, Y. Chen, X. Yang, H. Zhang and H. Niu, *Bioact. Mater.*, 2021, **6**, 433.

143 Y. Wang, M. Yang, J. Qian, W. Xu, J. Wang, G. Hou, L. Ji and A. Suo, *Carbohydr. Polym.*, 2019, **203**, 203–213.

144 K. Chen, C. Chang, Z. Liu, Y. Zhou, Q. Xu, C. Li, Z. Huang, H. Xu, P. Xu and B. Lu, *Colloids Surf., B*, 2020, **194**, 111166.

145 Y. Liu, X. Dai, B. Yu, M. Chen, N. Zhao and F.-J. Xu, *Biomater. Sci.*, 2022, **10**, 2618–2627.

146 D. Shao, Q. Gao, Y. Sheng, S. Li and Y. Kong, *Int. J. Biol. Macromol.*, 2022, **202**, 37–45.

147 D. Wei, Y. Xue, H. Huang, M. Liu, G. Zeng, Q. Wan, L. Liu, J. Yu, X. Zhang and Y. Wei, *Mater. Sci. Eng., C*, 2017, **81**, 120–126.

148 M. Xu, J. Qian, A. Suo, H. Wang, X. Yong, X. Liu and R. Liu, *Carbohydr. Polym.*, 2013, **98**, 181–188.

149 Q. Ren, Z. Liang, X. Jiang, P. Gong, L. Zhou, Z. Sun, J. Xiang, Z. Xu, X. Peng, S. Li, W. Li, L. Cai and J. Tang, *Int. J. Biol. Macromol.*, 2019, **130**, 845–852.

150 J. Pang, H. Xing, Y. Sun, S. Feng and S. Wang, *Biomed. Pharmacother.*, 2020, **125**, 109861.

151 Y. Song, H. Cai, T. Yin, M. Huo, P. Ma, J. Zhou and W. Lai, *Int. J. Nanomed.*, 2018, **13**, 1585.

152 B. Lu, F. Xiao, Z. Wang, B. Wang, Z. Pan, W. Zhao, Z. Zhu and J. Zhang, *ACS Biomater. Sci. Eng.*, 2020, **6**, 4106–4115.

153 T. A. Debele, L. Y. Yu, C. S. Yang, Y. A. Shen and C. L. Lo, *Biomacromolecules*, 2018, **19**, 3725–3737.

154 S. J. Lee and Y. Jeong, *J. Mater. Chem. B*, 2018, **6**, 2851–2859.

155 M. Li, Y. Zhao, J. Sun, H. Chen, Z. Liu, K. Lin, P. Ma, W. Zhang, Y. Zhen, S. Zhang and S. Zhang, *Carbohydr. Polym.*, 2022, **288**, 119402.

156 Y. Zhou, C. Chang, Z. Liu, Q. Zhao, Q. Xu, C. Li, Y. Chen, Y. Zhang and B. Lu, *Langmuir*, 2021, **37**, 2619–2628.

157 B. Chen, J. Cao, K. Zhang, Y. N. Zhang, J. Lu, M. Z. Iqbal, Q. Zhang and X. Kong, *J. Biomater. Sci. Polym. Ed.*, 2021, **32**, 2028–2045.

158 S. H. Choi, D. Y. Lee, S. Kang, M. K. Lee, J. H. Lee, S. H. Lee, H. L. Lee, H. Y. Lee and Y. Jeong, *Int. J. Mol. Sci.*, 2021, **22**, 6347.

